Electronic Supplementary Material (ESI) for Energy & Environmental Science.

Rewiring photosynthesis: Photosystem I-hydrogenase chimera makes H_2 *in vivo*

Andrey Kanygin[a], Yuval Milrad[b], Chandrasekhar Thummala[a,c], Kiera Reifschneider[a†], Patricia Baker[a], Pini Marco[b], Iftach Yacoby[b]* and Kevin E. Redding[a]*

[a.] *School of Molecular Sciences, Arizona State University, Tempe, Arizona, USA.*
[b.] *School of Plant Sciences and Food Security, Tel Aviv University, Tel Aviv, Israel.*
[c.] *Department of Environmental Science, Yogi Vemana University, Kadapa, Andhra Pradesh, India.*
† *Current address: 3582 AB Utrecht, Netherlands.*
*Corresponding authors.
Email: kredding@asu.edu ORCID:0000-0003-2819-4022 and Iftachy@tauex.tau.ac.il ORCID: 0000-0003-0177-0624

Content:

Supplementary materials and methods

Dissolved O_2 measurements *in vivo*

Dissolved O_2 was monitored with a Firesting O_2 optical oxygen meter (PyroScience). Cells were washed with either fresh TAP or TBP twice, then resuspended at approximately 5 µg Chl ml^{-1}. They were dark adapted and sparged with filtered water-saturated air for 10 min before the run. Each run made use of 2 ml of cell suspension stirred continuously in a 5-ml cuvette. For light-dependent O_2 evolution rates, the dark O_2 consumption rate (the average of rates in the dark just before and after illumination) was subtracted from the net evolution rate in the light. For maximal O_2 evolution rates, the cell suspensions (in TBP) were subjected to a 5-min dark period in the presence of 0.2 mM Phenyl-*p*-benzoquinone (PPBQ; Acros Organics), followed by 5 min of high red light (~2300 µmol photons m^{-2} s^{-1}) and 5 min of darkness.

$NADP^+$ photoreduction assay

The reaction mixture (2 mL) consisted of 10 mM sodium ascorbate (Sigma), 17 µM plastocyanin (Pc: prepared in-house from a recombinant source as described in ref. [1]), 3 µM ferredoxin (Fd: prepared in-house from a recombinant source as previously described [2]), 0.2 µM FNR (prepared in-house from a recombinant source as previously described [2]), 2.5 mM $NADP^+$ disodium salt (Roche), and 27 nM PSI in reaction buffer (50 mM Tris-HCl, pH 7.4, 3.35 mg mL^{-1} BSA, 10 mM $MgCl_2$, 200 mg mL^{-1} sucrose, 0.03% ß-DDM). The concentrations of Pc, Fd, and FNR were optimized for maximal reaction rates with WT PSI. Each sample was mixed in a 3-mL quartz cuvette with a stir bar for 3 minutes. All preparatory steps were done in the dark. The reference cuvette contained all components except PSI. Absorbance at 340 nm was measured with a Perkin Elmer Lambda35 double-beam spectrophotometer. Band pass filters (340 nm, 27nm FWHM, Omega Optical) were placed before the detectors to block actinic light. A red LED light source (630 nm, 300 µmol photons m^{-2} s^{-1}) was assembled on top of the cuvette and controlled manually. A technical replicate consisted of a "dark" run of 3 minutes using a data collection frequency of 6 Hz, followed by 3 min of data collected with the actinic light on. The data were analyzed for each run separately; each "dark" slope was subtracted from the following "light" slope to obtain a light-dependent rate before averaging. The dark rates never exceeded 11% of the light rates. An initial rate was determined from the slope of the line (linear fit with the instrumental weighting of error) to the first 9 points of each averaged data set using Beer's law and the extinction coefficient for NADPH at 340 nm (6.22 mM^{-1} cm^{-1}) with a path length of 1 cm.

Flavodoxin photoreduction assay

Recombinant *Synechococcus* sp. PCC7002 flavodoxin was prepared as previously described.[3] The reaction mixture consisted of ~100 nM PSI particles in 25 mM Tricine-KOH (pH 8), 50 mM $MgCl_2$, 20 mM KCl, 0.03 % ß-DDM, 5 mM sodium ascorbate, 5 µM Pc, and 5 µM flavodoxin. All preparation steps were performed in the dark. Accumulation of flavodoxin semiquinone was monitored with a JTS-10 kinetic spectrometer (Bio-Logic) using 10-µs flashes centered at 573 nm (6 nm full width at half maximum). Actinic light consisted of 250-ms LED pulses at 630 nm (3000 µmol m^{-2} s^{-1}), with the probe flash occurring 50 ms after the actinic pulse ceased, allowing time for any rapid decay processes to be complete. (This 250-ms/50-ms duty cycle was factored in the rate calculations.) An extinction coefficient of 5100 M^{-1} cm^{-1} for the flavosemiquinone-minus-flavin difference at 573 nm was used, based on the published difference spectrum of *Synechococcus* sp. PCC7002 flavodoxin. [4] The slow baseline drift in the dark was subtracted from the rate in the light to yield the light-dependent rate.

O_2 uptake assay

Reaction mixtures were prepared as in the flavodoxin photoreduction experiment, except that 2,6-dichlorophenol indophenol (0.2 mM) was used as mediator instead of Pc, and flavodoxin was not added. Dissolved O_2 was measured with a Clark-type electrode. Each sample was mixed in the dark to saturate with air. Data was collected with 1 Hz frequency for 1 minute in the dark, followed by 2 minutes under saturating illumination from a white LED (1200 µmol m^{-2} s^{-1} of PAR). Rates of O_2 consumption/production in the light were calculated for each replicate (n=3) via linear regression of 10-s intervals. The dark rate for each replicate was calculated from the last 2 minutes of the 3-min dark run of the sample before illumination commenced. This dark rate was subtracted from the light rate to determine the light-dependent rate, which was normalized to the amount of photobleachable P_{700}. The dark rate never exceeded 18% of the corresponding light rate. After data collection, the Chl content of each sample was measured to ensure consistency between replicates.

***In vivo* P_{700} photobleaching and fluorescence measurements**

Cells were collected during early log phase, centrifuged (3500 *x g* for 5 min) and resuspended to a Chl concentration of 33 µg mL^{-1} (P_{700}) or ~9 µg mL^{-1} (fluorescence) in 20% Ficoll™ PM400 (GE Healthcare), 10 mM sodium phosphate (pH 7.2). P_{700} bleaching and recovery was performed essentially as previously described.[5] Absorbance changes at 695 nm were measured with the JTS-10 spectrometer. For P_{700} photobleaching, actinic light (630 nm) was briefly (200 µs) switched off for each 10-µs detection measurement during the 10-s illumination period, followed by the dark decay.
For fluorescence, cells were dark adapted for 5 min before taking each measurement. (During dark periods, samples were sparged with air to prevent development of anoxia.) Fluorescence emission from Chl was measured with the JTS-10 Fluo59 accessory. A saturating pulse (80 ms, 8 mmol photons m^{-2} s^{-1}, 520 nm) was used to obtain F_{max}, measured 170 µs after the pulse. The steady-state fluorescence parameter (F_s) was measured after 2 minutes of illumination (520 nm) with actinic light of variable intensities. Quantum yields of PS II ($\Phi_{(II)}$) were calculated as described.[6]

Long term H_2 production in a photobioreactor (PBR)

Cells were grown in 4 L TAP under ambient room light (~5 µmol m^{-2} s^{-1} photosynthetically active radiation (PAR)) with constant air-sparging and stirring. They were harvested in the mid log-phase, resuspended in ~500 mL fresh TAP to OD_{735} ≈ 0.7 (corresponding to ~30 µg/mL of Chl) and transferred to the 400-mL PBR vessel. Once in the FMT150 PBR (see above), the culture was continuously sparged with Ar at 80 mL min^{-1}, controlled at the influx and monitored at the efflux by mass flow controllers (MC-500SCCM-D/5M, Alicat Scientific, USA). After 2 h of anaerobic adaptation in the dark, the culture was illuminated continuously with white light at 600 µmol photons m^{-2} s^{-1} PAR. Sterile argon was hydrated by bubbling through water and then through the sterile TAP media, before it entered the PBR vessel. The PBR was operated in turbidostat mode with OD_{735} set to remain between 0.60 and 0.65; Ar-sparged sterile TAP was used to dilute the culture, which was constantly stirred. The PBR gas efflux was passed through a 500-mL trap flask (to retain excess culture) before passing out and through the monitoring mass flow controller. A rubber septum mounted atop the trap flask allowed probing of the efflux gas with an air-tight syringe (100 µL, Hamilton), followed by injection of the sample into the GC-TCD, as in the experimental section.

Supplementary text

P_{700} photobleaching and recovery in thylakoid membranes

A saturating laser flash was used to trigger charge separation and creation of the $P_{700}^{+}(F_A/F_B)^{-}$ charge-separated state in <10 ns; [7,8] photo-induced bleaching of P_{700} and its recovery were monitored with 10-µs LED flashes. The fast component is attributed to charge recombination of the $P_{700}^{+}(F_A/F_B)^{-}$ state, which has a decay time of 40-200 ms, whereas the preceding $P_{700}^{+}F_X^{-}$ state recombines in 0.5-1 ms.[9] The slower decay is attributed to reduction of P_{700}^{+} by ascorbate in the fraction of photosystems in which the electron on F_A/F_B escaped to an exogenous acceptor (*e.g.* O_2) and is commonly seen.[10] Charge recombination from the iron sulfur cluster of hydrogenase domain of the chimera doesn't occur when oxygen is present as over 50% of electrons escape ETC and must be replenished by ascorbate. The fitting parameters are reported in **Table S1**.

For the experiment shown in **Figure S4**, essentially the same analysis was done, but it was performed on purified PSI^{H6} and PSI^{H6}-HydA2 that had been prepared and loaded into the cuvette anoxically.

Supplementary tables

Table S1. Fitting parameters of P_{700}^+ decay in thylakoid membranes

parameter	PSI	PSI-hydrogenase	Comments
τ_1	91 ± 5.6 ms	79 ± 12	Decay constant of fast phase (ms)
A_1	33 ± 0.7 %	30 ± 1.5 %	Amplitude of fast phase (% of total)
τ_2	5500 ± 150 ms	4500 ± 290	Decay constant of slow phase (ms)
A_2	60 ± 0.6 %	51 ± 1.3 %	Amplitude of slow phase (% of total)
A_0	6 ± 0.4 %	15 ± 0.8 %	Non-decaying fraction (% of total)
R^2	0.9993	0.9961	Coefficient of determination

Table S1. Bi-exponential fitting parameters of P_{700}^+ decay curves *in vitro* shown in Fig. 3A. Function: $A(t) = A_0 + A_1 \exp(-x/t_1) + A_2 \exp(-x/t_2)$. Fast recovery phase parameters τ_1 and A_1 are likely due to charge recombination from P_{700}^+ (F_A/F_B^-) while τ_2 and A_2 result from a slow reduction of P_{700}^+ by ascorbate.

Supplementary figures

MAHIVKIYDTCIGCTQCVRACPLDVLEMVPWGGATATDAVPHWKLALEELDKPKDGGRKVLIAQVAPAVRV
AIAESFGLAPGAVSPGKLATGLRALGFDQVFDTLFAADLTIMEEGTELLHRLKEHLEAHPHSDEPLPMFTSCCP
GWVAMMEKSYPELIPFVSSCKSPQMMMGAMVKTYLSEKQGIPAKDIVMVSVMPCVRKQGEADREWFCVSEP
GVRDVDHVITTAELGNIFKERGINLPELPDSDWDQPLGLGSGAGVLFGTTGGVMEAALRTAYEIVTKEPLPRL
NLSEVRGLDGIKEASVTLVPAPGSKFAELVAERLAHKVEEAAAAEAAAAVEGAVKPPIAYDGGQGFSTDDGK
GGLKLRVAVANGLGNAKKLIGKMVSGEAKYDFVEIMACPAGCVGGGGQPRSTDKQITQKRQAALYDLDERN
TLRRSHENEAVNQLYKEFLGEPLSHRAHELLHTHYVPGGASQMASAPRTEDCVGCKRCETACPTDFLSVRVY
LGSESTRSMGLSY

Figure S1. Coding sequence of the PsaC-HydA2 fusion polypeptide. Highlighted residues indicate the PsaC fragments (green), N-terminal junction (cyan), and C-terminal junction (red). The red highlighted Ala residue is shared between the HydA2 and PsaC sequences.

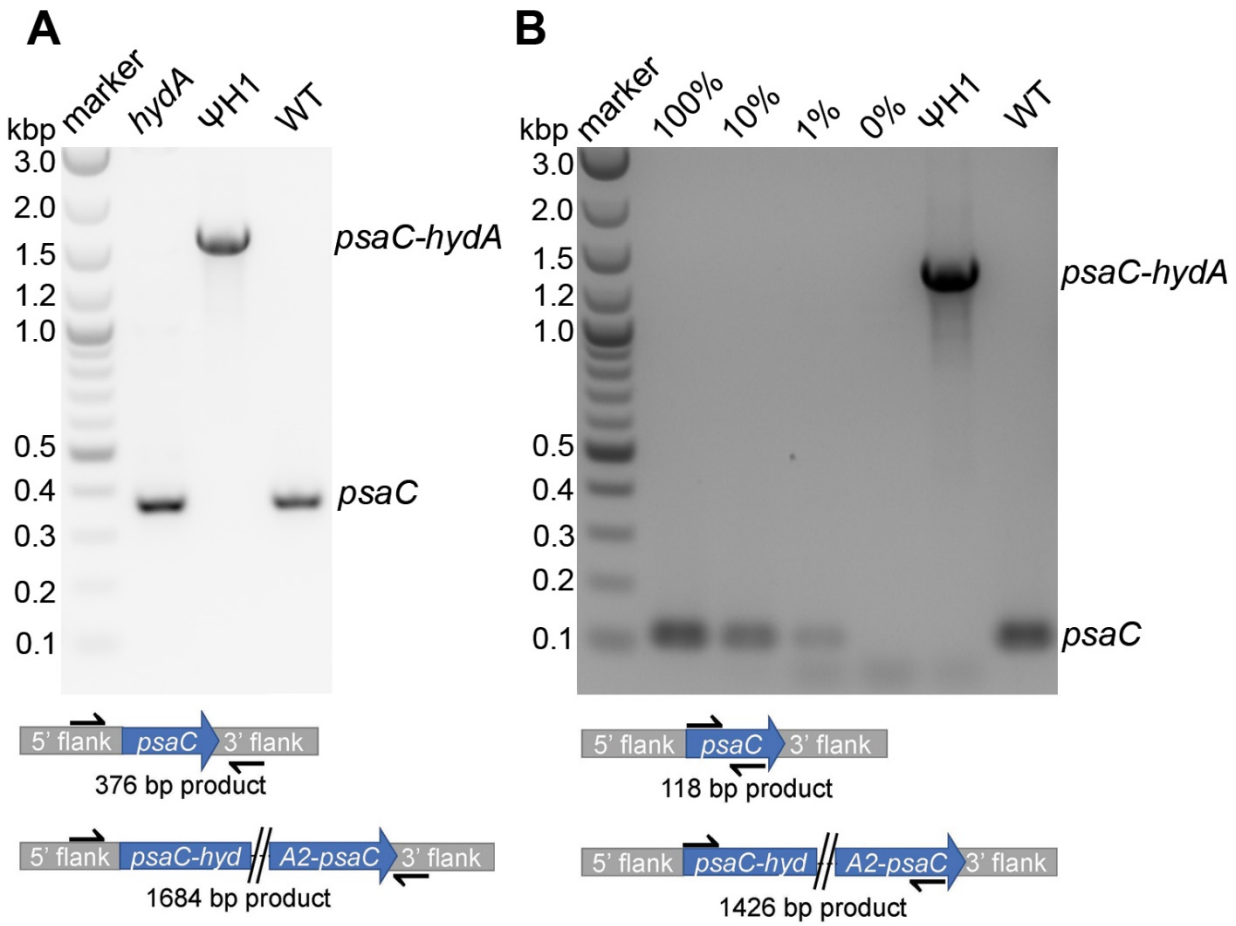

Figure S2. Agarose gel of PCR amplification of *C. reinhardtii* genomic DNA from parental (*hydA*), chimera-expressing (ΨH1) and WT strains with locus-specific (A) and gene-specific primers (B) **A:** *psaC* detection PCR with primers annealing to flanking sequences and corresponding cartoon showing primer locations and amplicon sizes using *psaC* or *psaC-hydA2* as the template. **B:** Homoplasmy detection PCR with gene-specific primers and corresponding cartoon with primer locations and amplicon sizes. Percentages indicate the abundance of the wild type genomic DNA (containing *psaC* gene) that had been diluted into the genomic DNA of the *psaCΔ* strain at the same DNA concentration (i.e., total genomic DNA was kept at 100 ng/reaction). PCR amplicons were resolved on 1% agarose gel and stained with ethidium bromide. A 2-log DNA marker (NEB) was used for size approximation; sizes in kbp are indicated to the left of the gel images.

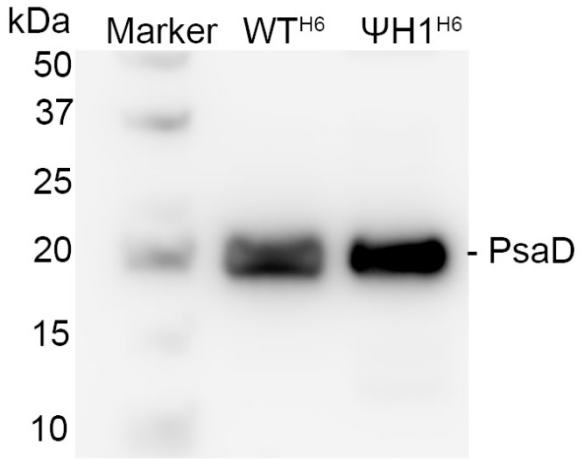

Figure S3. Immunoblot of isolated PSI particles using anti-PsaD antibodies. Samples were loaded on equal P_{700}, as in Figure 2. Integration of the anti-PsaD cross-reactive bands gave a ratio of 1.00:1.02 (PSI : PSI-HydA).

A

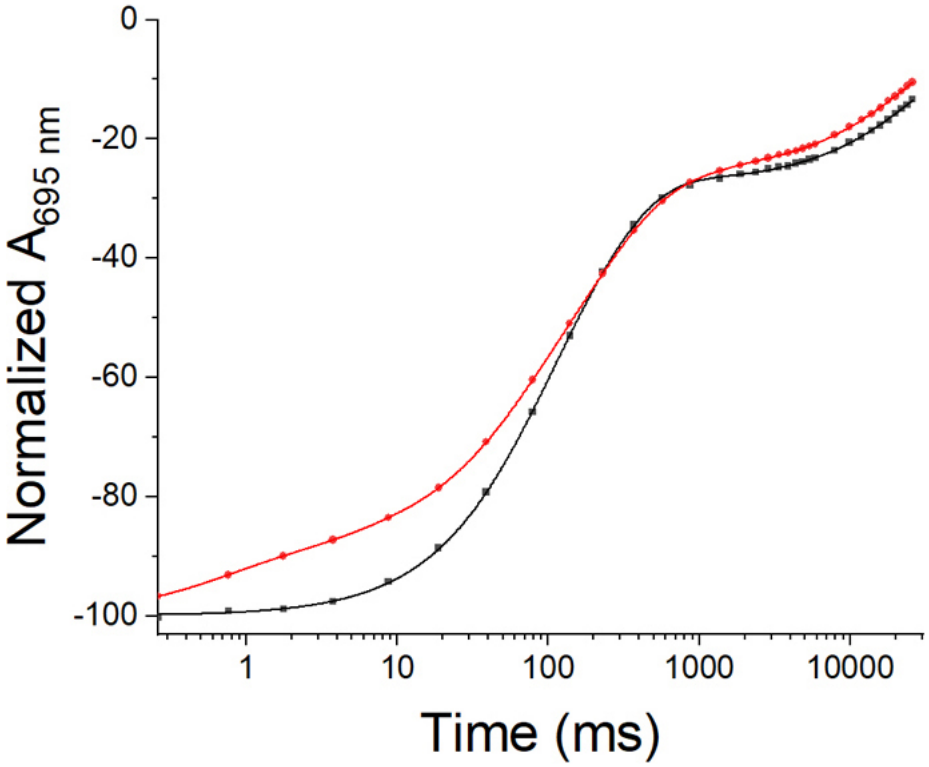

B

Assignment of phase	Time constant ± SE, ms (relative amplitude, %)	
	PSI^{H6}	**PSI^{H6}-HydA2**
CR of $P_{700}^{+}F_X^{-}$	N/A	0.56 ± 0.10 (7.3) 3.0 ± 0.6 (4.6)
CR of $P_{700}^{+}(F_AF_B)^{-}$	63 ± 4 (28.1) 204 ± 7 (44.5)	45 ± 3 (17.5) 192 ± 15 (35.8)
CR of $P_{700}^{+}F_H^{-}$	N/A	570 ± 81 (9.1)
ascorbate	30,000 ± 2750 (24.1)	25,500 ± 1060 (23.9)
Non-decaying	– (3.3)	– (1.8)
R^2	0.9999	0.9999

Figure S4. Spectroscopic characterization of anoxically prepared PSI^{H6} and PSI^{H6}-HydA2 particles that were loaded into a sealed cuvet in an anaerobic glovebox to eliminate O_2 from the environment. **(A)** Normalized transients (n=3, technical replicates) of P_{700}^{+} recovery upon laser flash-induced bleaching in anoxically prepared PSI particles: WT^{H6} (black, 74 fmol of P_{700}^{+}) and PSI^{H6}-HydA2 (red, 71 fmol of P_{700}^{+}). Solid lines represent fit to a multi-exponential decay, using the time constants and relative amplitudes reported in panel **B**. CR = charge recombination, F_H = [4Fe-4S] cluster of HydA2 domain

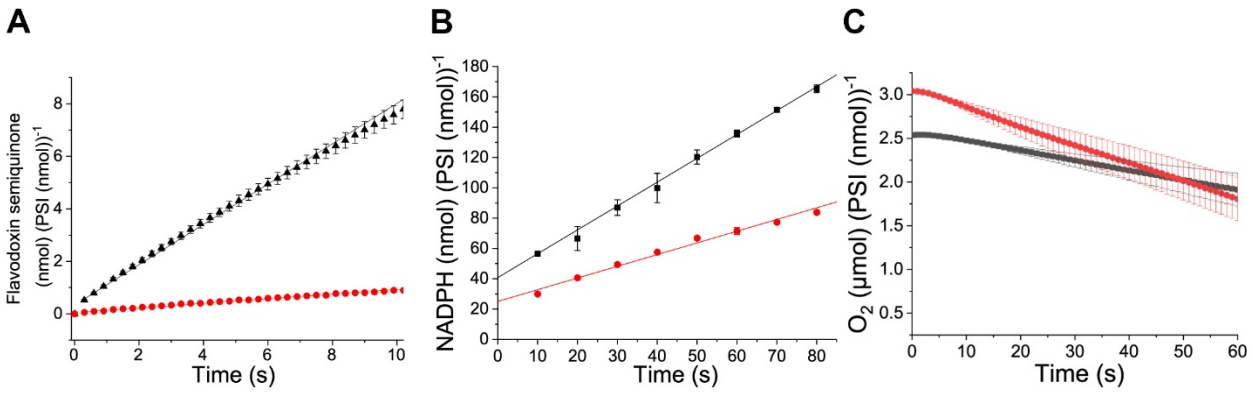

Figure S5. *In vitro* PSI activity measured by photoreduction of flavodoxin (**A**), $NADP^+$ (**B**) and O_2 (**C**). (**A**) Flavodoxin photoreduction with purified PSI [black=*hydA*, red=ΨH1] (normalized to 1 nmol of PSI) under saturating light conditions. Turnover rates are 0.77 s^{-1} (*hydA*) and 0.088 s^{-1}(ΨH1). (**B**) Assays contained equal amounts of PSI (54 nM) [black=WT^{H6}, red=$ΨH1^{H6}$] with an excess of ferredoxin (3 µM), FNR (0.2 µM), and $NADP^+$ (2.5 mM). Illumination (300 µmol of red photons m^{-2} s^{-1}) of cuvette commenced at t = 0. Lines represent a linear fit of the data. Rates thus obtained are 1.57 ± 0.01 and 0.77 ± 0.04 NADPH s^{-1} per PSI for WT and PSI-HydA, respectively. (**C**) O_2 reduction rates measured with a Clark-type electrode. The O_2 uptake rates were normalized to the amount of P_{700}. Maximal light-dependent rates were 12.7 ± 1.6 and 26.4 ± 4.8 O_2 s^{-1} per PSI for WT and PSI-HydA, respectively. Error bars represent SE (n=3).

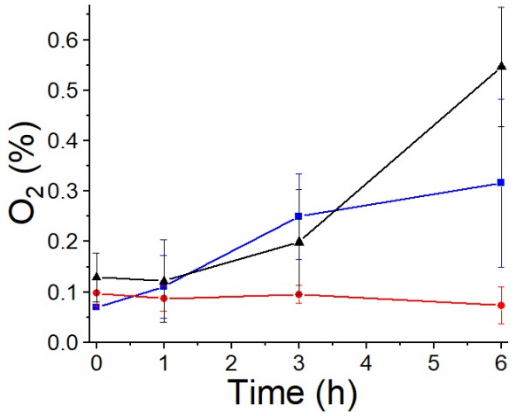

Figure S6. Accumulation of O_2, as measured by GC-TCD, in the headspace of sealed bottles containing cultures of WT (blue), *hydA* (black), and ΨH1 (red). Illumination intensity was 200 µmol photons m^{-2} s^{-1}. Experiment is the same one as shown in Fig. 4B.

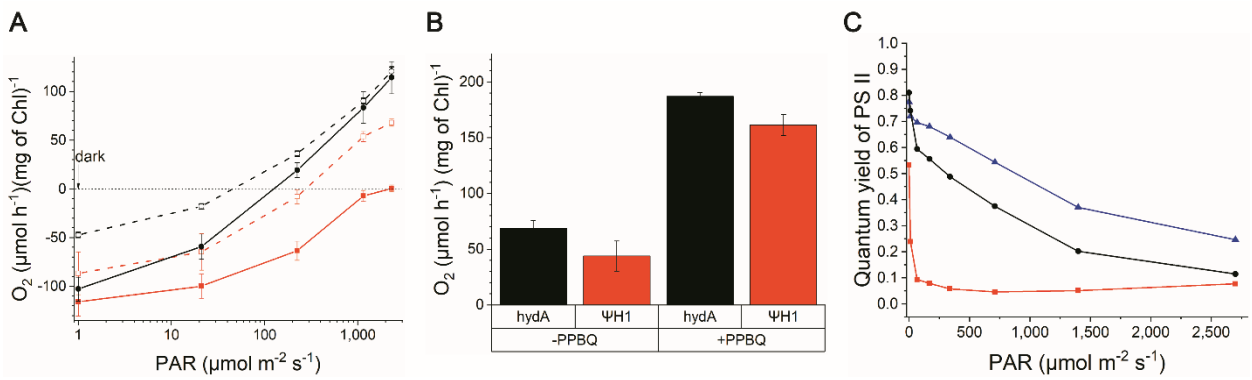

Figure S7. Rates of dissolved O_2 consumption/production and quantum yield of PSII. **A**: Net O_2 production rates under red LED illumination in aerobic cultures of *hydA* (black, circles) or ΨH1 (red, squares) in media with (solid lines and symbols) or without (dashed lines, hollow symbols) acetate. Data at 1 PAR correspond to the dark sample for graphing purpose. **B**: Light-dependent O_2 evolution rates under ~2300 µmol m^{-2} s^{-1} of red light in cultures containing bicarbonate, with or without addition of 0.2 mM PPBQ. In all instances, cells were grown in medium containing acetate and then resuspended in fresh medium containing bicarbonate instead of acetate as a carbon source before being placed into the measuring cuvette. Cells were stirred and occasionally bubbled with air to maintain them in an aerobic state before dissolved O_2 was measured with an optical sensor. Error bars represent standard error (n=3). **C**: Quantum yield of PSII in WT (blue), *hydA* (black) and ΨH1 (red) strains under various illumination intensities. Cells were aerobically resuspended in 20% Ficoll buffer (Tris-phosphate, pH 7.0) and kept aerobic throughout the experiment.

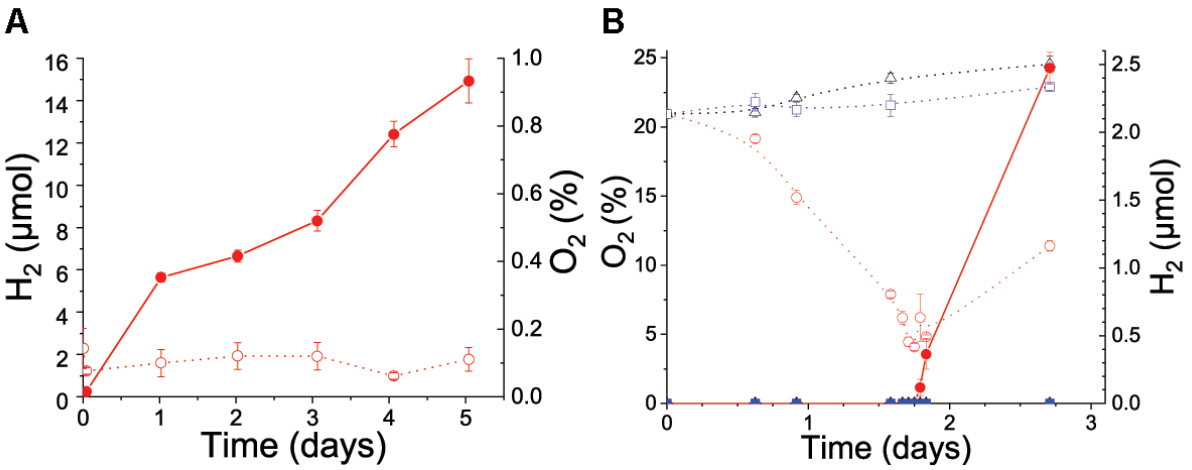

Figure S8. Long-term measurements of H_2 (solid symbols and lines) and O_2 (hollow symbols, dotted lines) produced by 10-mL cultures in sealed 25-mL bottles with (**A**) or without (B) prior imposition of anoxia via argon-sparging. ΨH1 (red), *hydA* (black) or WT (blue) cultures resuspended at ~1 µg/mL of Chl in fresh TAP were exposed to white light (~200 µmol m^{-2} s^{-1} PAR) and the headspace (15 mL) was sampled at the indicated times, followed by analysis via GC-TCD. Error bars represent SE (n=3).

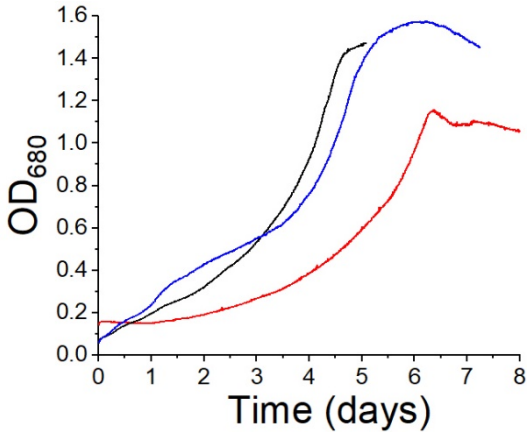

Figure S9. Photoautotrophic growth of *hydA* (black), WT (blue), and ΨH1 (red) cultures in a closed photobioreactor in TBP medium containing bicarbonate as the sole carbon source. Growth was monitored at 680 nm. The cultures were sparged in the dark with N_2 for 1 h prior to growth under illumination (340 µmol photons m^{-2} s^{-1}).

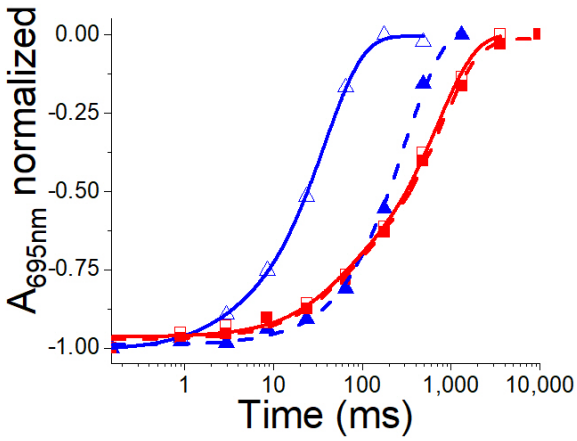

Figure S10. Cyclic electron flow measured in WT and ΨH1 cells. Normalized P_{700}^{+} decay transients after 10 s of strong illumination (940 µmol photons m^{-2} s^{-1}) in fully aerobic cultures of WT (blue triangles) and ΨH1 (red squares), to which had been added 20 µM DCMU (empty symbol/solid line), or 20 µM DCMU + 20 µM 2,5-dibromo-3-methyl-6-isopropylbenzoquinone (DBMIB; filled symbol/dashed line). The level of P_{700} photobleaching is normalized to the maximal level, and is plotted on a log time scale. Note that the rate of P_{700}^{+} reduction in the absence of PSII (with DCMU) is much slower in ΨH1 than in the WT cells and is unaffected by inhibition of cytochrome b_6f (with DBMIB), unlike the WT cells. Taken together, this indicates that cyclic electron flow is negligible in ΨH1 cells.

Supplementary references

1 S. Kuhlgert, F. Drepper, C. Fufezan, F. Sommer and M. Hippler, *Biochemistry*, 2012, **51**, 7297–7303.

2 P. Marco, M. Kozuleva, H. Eilenberg, Y. Mazor, P. Gimeson, A. Kanygin, K. Redding, I. Weiner and I. Yacoby, *Biochim. Biophys. Acta - Bioenerg.*, 2018, **1859**, 234–243.

3 J. Zhao, R. Li and D. A. Bryant, *Anal. Biochem.*, 1998, **264**, 263–270.

4 K. Meimberg and U. Mühlenhoff, *Photosynth. Res.*, 1999, **61**, 253–267.

5 J. Alric, J. Lavergne and F. Rappaport, *Biochim. Biophys. Acta - Bioenerg.*, 2010, **1797**, 44–51.

6 B. Genty, J.-M. Briantais and N. R. Baker, *Biochim. Biophys. Acta - Gen. Subj.*, 1989, **990**, 87–92.

7 N. Fischer, P. Sétif and J. D. Rochaix, *J. Biol. Chem.*, 1999, **274**, 23333–23340.

8 K. Brettel and W. Leibl, *Biochim. Biophys. Acta - Bioenerg.*, 2001, **1507**, 100–114.

9 K. Brettel, *Biochim. Biophys. Acta - Bioenerg.*, 1997, **1318**, 322–373.

10 R. Jordan, U. Nessau and E. Schlodder, in *Photosynthesis: Mechanisms and Effects*, ed. G. Garab, Springer Netherlands, Dordrecht, 1998, pp. 663–666.